

Motions of single and a group of particles with different shapes flowing down in fixed bed channels

Yuya Takakuwa

Graduate School of Science and Engineering, Chuo University
1-13-27 Kasuga, Bunkyo-ku, Tokyo 112-8551, Japan
Tel. +81 (03) 3817 1615

Email: takakuwa0715@civil.chuo-u.ac.jp

Shoji Fukuoka

Research and Development Initiative, Chuo University
1-13-27 Kasuga, Bunkyo-ku, Tokyo 112-8551, Japan
Tel. +81 (03) 3817 1625

Email: sfuku@tamacc.chuo-u.ac.jp

Gravel-bed rivers are composed of particles with various shapes and sizes. In this paper, the image analysis of laboratory experiments of single gravel motions in flows and numerical simulations were conducted. Effects of particle shapes on sediment transport mechanism were discussed.

Particles were transported in characteristic manners depending on their shapes. Spheres rolled, on the other hand, non-spherical particles moved by saltation and rolling. Velocities of single particles were influenced by shapes more than sizes and became large as they deviated from sphere shape. Motions of non-spherical particles varied in the vertical direction, so the interaction among non-spherical particles became smaller than that of spheres. Further, the group velocity of mixed particles was estimated by average velocities of single particles and average velocity deceleration rates of a group of particles.

Key Words: gravel-bed rivers, sediment transport, interaction among particles, particle shape

1. Introduction

Understanding of sediment transport mechanism in gravel-bed rivers is insufficient because transportation experiments of gravels with various shapes and sizes are complicated in comparison with those of sands. Therefore, effects of particle shapes and sizes on transport mechanism should be examined in detail.

In recent years, the progress of computing performance has made possible to analyze three-dimensional flow motions and particle motions by the Euler-Lagrange approach [1]. Fukuoka et al. [2] developed the numerical movable-bed channel expressing motions of flow and particles with various shapes and sizes, and emphasized the importance of considering particle shapes on transport mechanism of a group of particles as well as a single particle.

In this paper, to clarify fundamental effects of particle shapes on motions of single and a group of particles, following investigations were conducted. First, Euler-Lagrange simulations were applied to motions of single gravels with different shapes and sizes in the laboratory experiments conducted by Shigemura [3] and Fukuoka et al. [4]. Particle motions in the numerical channel were compared with the results of the laboratory experiments. Second, transportations of single particles (4 shapes and 3 sizes) were simulated and effects of particle shapes on motions of single particles were examined. Third, transportations of a group of particles were simulated and effects of particle shapes and interactions among particles on motions of a group particles were discussed.




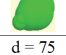
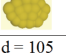
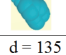
2. Comparisons of laboratory experiment results and numerical simulations

2.1. Conditions of experiments and numerical simulations

To clarify transport mechanism of single gravels with different sizes, Shigemura [3] and Fukuoka et al. [4] photographed motions of single gravels (see Table 1) in an open channel flow and analyzed them. Figure 1 shows conditions of the experimental channel with 45 m long, 1 m width, 1:20 bed slope and 0.5 m³/s discharge. The channel cross-section was a broad concave shape.

In the numerical simulations, model particles (see Table 1) were transported by water in the numerical channel. The length of the numerical simulation channel was 38 m. The discharge 0.5 m³/s was supplied

Table 1. Gravels used for the laboratory experiments and model particles for the numerical simulations.

Shape type	Ellipsoid-type	Disk-type	Pear-type
Gravel			
Model particle			
size (mm)	d = 75	d = 105	d = 135

*Particle size is defined as the diameter of a sphere with equivalent volume.

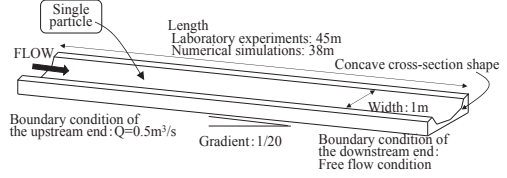


Fig. 1. Conditions for the experimental channel and the numerical simulation channel.

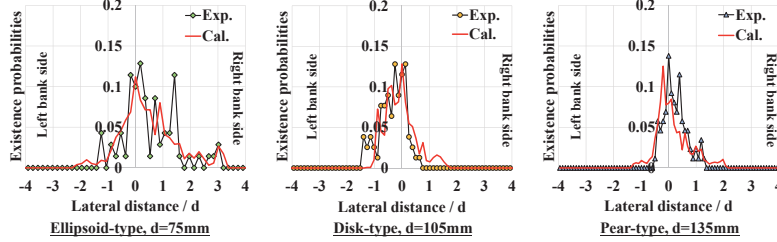


Fig. 2. Lateral distributions of existence probability density of single particles.

Table 2. Average velocities of single particles.

Average velocity	Ellipsoid-type d=75mm	Disk-type d=105mm	Pear-type d=135mm
Exp. (m/s)	3.30	3.81	3.54
Cal. (m/s)	3.03	3.49	3.24

at the upstream end and the condition of the zero pressure at the downstream end was given.

2.2. Numerical method

The numerical method of Fukuoka et al. [2] was used for numerical simulations. In the numerical simulations, flow and particle motions were calculated by the Euler-Lagrange approach. Fluid motions are simulated by governing equations (1)-(4) of one-fluid model of the incompressible fluids:

$$\frac{\partial u_i}{\partial x_i} = 0 \quad (1) \quad \frac{\partial u_i}{\partial t} + u_j \frac{\partial u_i}{\partial x_j} = g_i - \frac{1}{\rho} \frac{\partial P}{\partial x_i} + \frac{\partial}{\partial x_j} \{2(v + \nu_i) S_{ij}\} \quad (2)$$

$$v_i = (C_s \Delta)^2 \sqrt{2 S_{ij} S_{ij}} \quad (3) \quad S_{ij} = \frac{1}{2} \left(\frac{\partial u_i}{\partial x_j} + \frac{\partial u_j}{\partial x_i} \right) \quad (4)$$

where u_i : i-direction mass averaged velocity within a fluid cell including particles, ρ : volume averaged density, g_i : i-direction gravitational acceleration, P : sum of the pressure and isotropic component of SGS stress, ν : kinematic viscosity, ν_i : SGS turbulent viscosity, S_{ij} : strain rate tensor, C_s : Smagorinsky constant and Δ : calculation grid size.

Particle motions are expressed by translational and rotational equations of rigid bodies. Fluid forces acting on particles are calculated by the second term and the third term in the right side of equation (2) and integrated them on the region of a particle. Contact forces and torques are evaluated by Distinct Element Method [5]. Model particles are made by superposing small spheres [6] as shown in Table 1.

2.3. Comparisons of the result of experiments and numerical simulations





Figure 2 shows probability distributions in the lateral direction of experimental and simulated single gravels. Simulated probability distributions almost agreed with the result of laboratory experiments in each case. Table 2 shows average velocities of the experiments and numerical simulations of single particles. Although average velocities of numerical simulations of single particles were about 8 % smaller than those of the experiment in all cases, the relative magnitude of average velocities of numerical simulations was almost the same as that of the experiments. We confirmed that the numerical simulations could reproduce well motions of single particles flowing down in the fixed-bed channel.

3. Effects of particle shapes on motions of single particles

Transportation simulations of single particles (4 shapes shown in Table 3: sphere, ellipsoid-type, pear-type and disk-type, 3 sizes: d = 75, 105, 135 mm) were conducted under the conditions described in Figure 1.

Figure 3 describes consecutive motions of single particles with different shapes plotted at every 0.1

Table 3. Characteristics of particle shapes.

Model particle				
Shape type	Sphere	Ellipsoid-type	Pear-type	Disk-type
Dimensionless long-axis (a/d)	1.00	1.39	1.34	1.50
Dimensionless middle-axis (b/d)	1.00	1.01	0.90	1.00
Dimensionless short-axis (c/d)	1.00	0.79	0.83	0.60
S.F. (Shape Factor) S.F. = c/\sqrt{ab}	1.00	0.67	0.76	0.49
*Dimensionless maximum projection area	1.00	1.21	1.25	1.61
* Dimensionless maximum projection area Maximum projection area = Projection area of a sphere with equivalent volume				

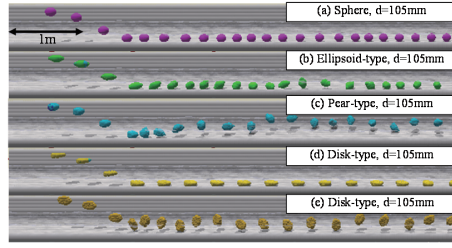


Fig. 3. Consecutive motions of single particles with different kinds of shapes.

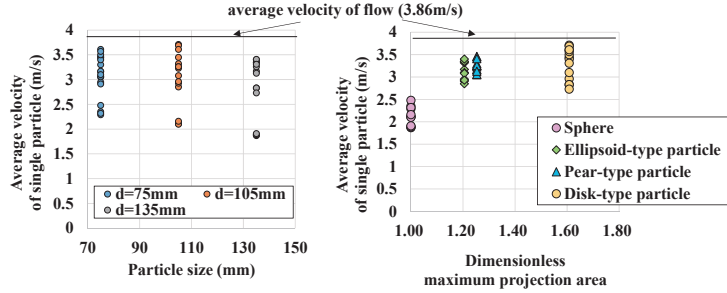


Fig. 4. Relations between average velocities versus sizes and shapes of single particles.

second. Naturally single particles were transported in characteristic manners depending on their shapes. Sphere (a) moved by rolling. Ellipsoid-type particle (b) and pear-type particle (c) moved by saltation and rolling taking the long-axis to a rotating-axis. Disk-type particle moved in two typical manners (gliding just above the bed (d) or rolling taking the short-axis to rotating-axis) and in a compound manner.

Figure 4 shows relations between particle velocities versus sizes and shapes. Average velocities of single particles varied between 2 ~ 4 m/s, and effects of sizes on particle velocities were not appreciated clearly. On the other hands, average velocities were considerably different by particle shapes. Average velocities of a disk-type particle became about one and a half as much as those of a sphere. A shape index of particles should be selected depending on the sedimentation subject. We chose the dimensionless maximum projection area as a shape index shown in Table 3 because many particles moved taking a large projection area against the flow. The maximum projection area controls particle motions as Sneed et al. [7] pointed out. Average velocities of single particles were influenced by shapes more than sizes and became large as the dimensionless maximum projection area increased.

4. Effects of particle shapes and interactions among particles on motions of a group of particles

Transportation simulations of single particles and 4 types of 24 particles (spheres, pear-type particles, disk-type particles and mixed particles of three different types, size: $d = 105$ mm) were performed in the rectangular channel of 21 m long, 2.2 m width and 1:100 bed slope shown in Figure 5. The $3.0 \text{ m}^3/\text{s}$ discharge was given at the upstream end and the zero pressure was imposed at the downstream end. The water depth was 0.44m and the Froud number was 1.4. Particles were given momentarily in the region of $4 < x < 5$ m, $-0.7 < y < 0.7$ m, $0 < z < 0.35$ m with the initial velocity of 2.5 m/s.

At first we discuss vertical distributions of existence probability density of single and a group of particles (see Figure 6). It was found that vertical distributions of existence probability density of a group of particles were almost equal to those of single particles. The moving height of particles was determined by the center of gravity of particles. Heights were different from shapes and became large as particle shapes deviated from the spherical shape.

Table 4 shows average velocities of single and a group of particles and average velocity deceleration rates (r_i ; see equation (5)) of particles group. Average group velocities to average velocities of single particles were less for spheres 13%, pear-type 11% and disk-type 8%. This demonstrated interactions between particle-particle and flow-particles. The reason was because individual particles composing a group of particles were affected by wakes of other particles and fluid forces acting on particles became small. The relation between particle velocities and vertical motions and interaction among particles was described as follows. As particles deviated from the spherical shape, they jumped to higher levels and then interactions among particles (average velocity deceleration rates: r_i) were reduced. Finally, the average velocity of mixed particles with three kinds of shapes was estimated by equation (6) using

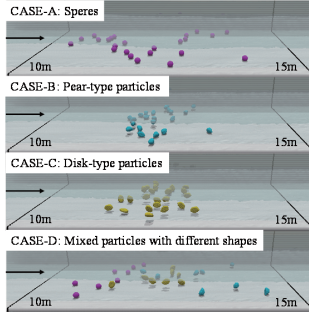


Fig. 5. Motions of a group of particles with different kinds of shapes.

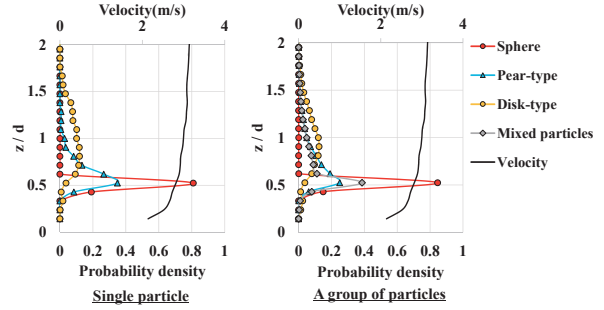


Fig. 6. Vertical distributions of existence probability density.

Table 4. Average velocity of single and a group of particles.

Average Velocity	Single particle: V_s (m/s)	A group of particles: V_m (m/s)	$r_i = \frac{V_s - V_m}{V_s}$
Sphere	1.59	1.39	0.13
Pear-type	2.28	2.03	0.11
Disk-type	1.96	1.81	0.08
Mixed particles	-	1.74	-

Average velocity deceleration rate: r_i

$$r_i = \frac{V_s - V_m}{V_s} \quad (5)$$

average velocities of respective single particles and average velocity deceleration rates expressing effects of interaction among particles

$$V_{mix} = \sum_{i=1}^n (1 - r_i) \alpha_i V_{si} \quad (6)$$

where V_{mix} : average group velocity of mixed particles, V_{si} : average velocity of i shape single particle, n : number of different particle shapes, α_i : mass rate of i shape particles and r_i : average velocity deceleration rate of i shape group of particles. The simulated velocity was 1.74 m/s and the velocity estimated by equation (6) was 1.73 m/s.

5. Conclusions

Main conclusions were described as follows:

1. Particles moved taking characteristic manner on their shapes in a flow. Spheres, for instance, moved by rolling, ellipsoid-type particles and pear-type particles moved by saltation or rolling taking the long-axis to a rotating-axis and disk-type particles moved by gliding and rolling taking the short-axis to a rotating-axis.
2. Average velocities of single particles were influenced by their shapes compared to their sizes. Dimensionless maximum projection area was used as the shape index because particles mainly moved taking a large projection area against the flow. Average velocities became large as dimensionless maximum projection area increased.
3. Average velocity deceleration rates of non-spherical particles expressing the interaction among them became smaller than that of spheres because non-spherical particles jumped to high levels. Average velocity of mixed particles with different kinds of shapes was estimated using average velocities of single particles and average velocity deceleration rates of respective shape of a group of particles.

References

- [1] Ushijima S., Fukutani A., and Makino O.: Prediction method for movements with collisions of arbitrary-shaped objects in 3D free-surface flows, *JSCE B Vol.64, No.2, pp.128-138, 2008 (in Japanese)*.
- [2] Fukuoka S., Fukuda T., and Uchida T.: Effects of sizes and shapes of gravel particles on sediment transports and bed variations in a numerical movable-bed channel, *Advances in Water Resources, Vol.72, pp.45-56, 2014*.
- [3] Shigemura K.: The movement mechanism of gravel flowing down a sediment flushing concrete channel and development of abrasion of the channel bed, *Master's thesis, Hiroshima University, 2004 (in Japanese)*.
- [4] Fukuoka S., Watanabe A., Shinohara Y., Yamashita S. and Saito K.: Movement mechanism for a mass of gravel flow with high speed and estimation of channel bed abrasion, *Advances in River Engineering, JSCE, Vol.11, 291-296, 2005 (in Japanese)*.
- [5] Cundall P. A. and Strack. O. D. L.: A discrete numerical model for granular assemblies, *Geotechnique, Vol.29, No.1, pp.47-65, 1979*.
- [6] Matsushima T., Katagiri J., Uesugi K., Tsuchiyama A., and Nakano Z.: 3D shape characterization and image-based DEM simulation of the lunar soil simulant FJS-1, *Journal of Aerospace Engineering, Vol.22, No.1, pp.15-23, 2008*.
- [7] E. D. Sneed, and R. L. Robert.: Pebbles in the lower Colorado River, Texas, a study in particle morphogenesis, *Journal of Geology Vol.66, pp.114-150, 1958*.